Case Study

Axial Skeletal Malformations in Genetically Modified *Xenopus laevis* and *Xenopus tropicalis*

Anne L Zlatow,[1] Sabrina S Wilson,[2] Donna M Bouley,[1] Joanne Tetens-Woodring,[3] Daniel R Buchholz,[4] and Sherril L Green[1,*]

Skeletal malformations in captive-bred, adult *Xenopus* spp., have not previously been reported. Here we describe 10 sexually mature, genetically modified laboratory frogs (6 *Xenopus laevis* and 4 *Xenopus tropicalis*) with axial skeletal abnormalities. The young adult frogs were described by veterinary staff as presenting with "hunchbacks," but were otherwise considered to be in good health. All affected frogs were genetically engineered using various techniques: transcription activator-like effector nucleases (TALEN) editing using thyroid hormone receptor α TALEN mRNA, restriction enzyme-mediated integration methods involving insertion of the inducible transgene pCAR/TRDN, or via *I-SceI* meganuclease transgenesis using either pDRTREdpTR-HS4 or pDPCrtTA-TREG-HS4 plasmid sequences. Radiographic findings (6 frogs) and gross necropsy (10 frogs) revealed vertebral column malformations and sacroiliac deformities that resulted in moderate to severe kyphosis and kyphoscoliosis. These findings were confirmed and additional skeletal abnormalities were identified using computed tomography to create a 3D reconstruction of 4 frogs. Additional findings visible on the 3D reconstructions included incomplete vertebral segmentation, malformed transverse processes, and a short and/or curved urostyle. Histopathologic findings included misshapen intervertebral joints with nonconforming articular surfaces, narrowed joint cavities, flattened or irregularly-formed articular cartilage, irregular maturation lines and nonpolarized chondrocytes, excess fibrocartilage, and evidence of irregular bone resorption and growth. While the specific etiology of the vertebral skeletal abnormalities remains unclear, possibilities include: 1) egg/oocyte physical manipulation (dejellying, microinjection, fertilization, etc.), 2) induction and expression of the transgenes, 3) inactivation (knockout) of existing genes by insertional mutagenesis, or 4) a combination of the above. Furthermore, the possibility of undetected changes in the macro or microenvironment, or a feature of the genetic background of the affected frogs cannot be ruled out.

Abbreviations: MBS, modified Barth's solution; NF, Nieuwkoop and Faber; REMI, restriction enzyme-mediated integration; SVL, snout-to-vent length; *THRA*, thyroid hormone receptor alpha; TALENs, transcription activator-like effector nucleases; *X. laevis*, *Xenopus laevis*; *X. tropicalis*, *Xenopus tropicalis*

Xenopus laevis (X. laevis) and *Xenopus tropicalis (X. tropicalis)* are important animal models for studies of toxicology, cancer, regenerative medicine, and vertebrate development.[2,4,7,19,29,31,38,47,48,50,51,53] Both species produce large numbers of oocytes and eggs that can be easily manipulated in the laboratory,[43,51] and thus readily lend themselves to transgenic technology.[7,10,13,14,22,36,45-47,50,52] However, most genetically modified *Xenopus* spp. are studied during the early stages of development and are not raised to sexual maturity.[23,53] Thus, descriptions of adult, genetically modified *Xenopus* spp. and their phenotypes, particularly concerning skeletal malformation, are rare.[12,14,36]

Kyphosis and scoliosis are axial skeletal deformities that result in abnormal curvature of the vertebral column. Kyphosis is defined as an abnormal dorsal curvature of the vertebral column; scoliosis is defined as an abnormal vertebral column curvature along the sagittal plane. Vertebral column abnormalities in embryonic *Xenopus* spp. have been attributed to heat shock[27] and exposure to various toxins; however, the *Xenopus* spp. in these investigations were not studied through sexual maturity.[3,21,24,41,53] Scoliosis in laboratory *X. laevis* has also been experimentally induced by unilateral removal of vestibular end organs at larval stages.[15] In addition, naturally occurring, spontaneous skeletal malformations have been sporadically reported in frogs and amphibians.[25,26,30,40] In these reports, the malformations were associated with nutritional factors, including calcium and vitamin D deficiencies[30] and parasite infestation.[25,26,40] In one report, wild-caught bullfrog (*Rana catesbeiana*) tadpoles bred in wetlands treated with wastewater were unable to tolerate the level of inorganic nitrogen pollution and subsequently developed scoliosis, calcinosis, and edema.[44]

Vertebral skeletal malformations, particularly scoliosis, have been well described in laboratory zebrafish (*Danio rerio*) and Atlantic salmon (*Salmo salar*) housed in tanks with a high stocking density,[33] hypoxic conditions,[11] or water with a low pH.[1,16] Dioxin exposure has been reported to contribute to scoliosis in juvenile laboratory zebrafish (*Danio rerio*) and to have transgenerational effects.[4] Vertebral column abnormalities, scoliosis

Species Sex (M/F)	Method of genetic modification	Description of manipulation
X. laevis F	REMI[30; 52]	F1 offspring of wild type female and male with pCAR/TRDN (inducible) transgene. This individual was briefly induced with doxycycline as a young tadpole.
X. tropicalis F	TALENs[14; 55]	Injected as a zygote with TALENs to disrupt *THRA*.
X. tropicalis F	TALENs[14; 55]	Injected as a zygote with TALENs to disrupt *THRA*.
X. tropicalis F	TALENs[14; 55]	Injected as a zygote with TALENs to disrupt *THRA*.
X. laevis M	Meganuclease[38; 41; 45]	Injected as a zygote with pDRTREdpTR-HS4 transgene. This transgene constitutively expresses red fluorescent protein in the lens of the eye.
X. laevis F	Meganuclease[38; 41; 45]	Injected as a zygote with pDPCrtTA-TREG-HS4 transgene. This transgene constitutively expresses green fluorescent protein in the lens of the eye.

Figure 1. Summary of genetic modifications known for 6 of the 10 affected frogs that were necropsied. The methodology used for 4 of the affected frogs from this cohort was not specified at the time of submission to necropsy.

in particular, have also been observed in *Ptk7* mutant zebrafish[20] in association with interrupted Notch, Wnt, or fibroblast growth factor signaling pathways.[20,32,42] Upregulation of VEGF in mutant laboratory mice has likewise resulted in scoliosis.[6] Although genetic manipulation of zebrafish, mice, and other laboratory species has resulted in skeletal malformations, genetic manipulation has not yet been identified as a cause of axial skeletal malformations in *Xenopus* spp.

In this current investigation, we report axial skeletal malformations in adult, genetically modified *X. laevis* and *X. tropicalis*. We describe the radiographic, gross, histopathologic, and computed tomography (CT) scan findings. The animals examined in this report were part of a larger colony of *Xenopus* spp., housed under standard laboratory conditions and maintained for the purpose of investigation into thyroid hormone receptor function and gene expression and regulation.[43]

Materials and Methods

Genetic Manipulation. These experimental protocols and conditions were approved by the University of Cincinnati's Institutional Animal Care and Use Committee. The purpose of this study was to examine the role of thyroid hormone receptors in gene regulation and metamorphosis.[7-9,13] Typically, this involved genetic engineering of frogs via transcription activator-like effector nucleases (TALENs) mediated editing by injecting embryos with thyroid hormone receptor α (*THRA*) TALEN mRNA,[13] restriction enzyme-mediated integration (REMI) methods involving insertion of the inducible transgene pCAR/TRDN,[10] or *I-SceI* meganuclease transgenesis using plasmid sequences pDRTREdpTR-HS4 or pDPCrtTA-TREG-HS4.[43] TALEN injections produced mosaic frogs because not all of the cells in their bodies contained mutant *THRA*. In REMI transgenic frogs, concatenated copies of pCAR/TRDN were likely present at several insertion sites in the genome;[37] induced expression of a dominant negative thyroid hormone receptor occurs only in

muscle cells, and then only after treatment with doxycycline. *I-SceI* meganuclease injections typically result in highly mosaic founders that exhibit lower copy numbers and fewer insertion sites in the genome as compared with REMI.[37] The transgenes pDRTREdpTR-HS4 or pDPCrtTA-TREG-HS4 cause constitutive expression of red or green fluorescent protein expression in the eye lens and can exhibit doxycycline-inducible expression of green fluorescent protein and a constitutively active mutant thyroid hormone receptor throughout the body. These manipulations were intended to disrupt pathways required for normal metamorphosis and frog development.

For TALEN injections, freshly fertilized *X. tropicalis* eggs were dejellied for 5 to 10 min in 3% L-cysteine (Sigma–Aldrich) in 0.1 × modified Barth solution (MBS). These eggs were then transferred to 3% Ficoll in 0.1 × MBS and injected with mRNA into one cell at the 2-cell stage. After 3 to 5 h, the surviving embryos were transferred to 0.01 × MBS.[13] Injections of *I-SceI* meganuclease for *X. laevis* followed a similar procedure.[43] REMI in *X. laevis* involved injecting a mixture of decondensed sperm nuclei, transgenesis plasmid, and restriction enzyme into ovulated, unfertilized eggs.[14] All injections, regardless of genetic modification methodology, were administered by trained personnel as follows: *X. tropicalis* injection volume 2 to 4 nL, and *X. laevis* injection volume 5 to 10 nL. The embryos do not survive injection of larger volumes. Figure 1 summarizes the methods used to generate 6 of the frogs described in this report. The 5 affected frogs described in Figure 1 were genetically manipulated as zygotes, using methods previously described.[13,28,36,39,49,52] The sixth affected frog, which had not been genetically manipulated as a zygote, was the offspring (F1) of phenotypically normal but transgenic parents (Figure 1). Transgenes in these parents were created by means of REMI.[28,49] The other affected frogs featured in Figure 1 were created by means of TALENs[46,52] or meganuclease,[36,39] as described. The appearance of this phenotype was not anticipated with any of these transgenes or knockout
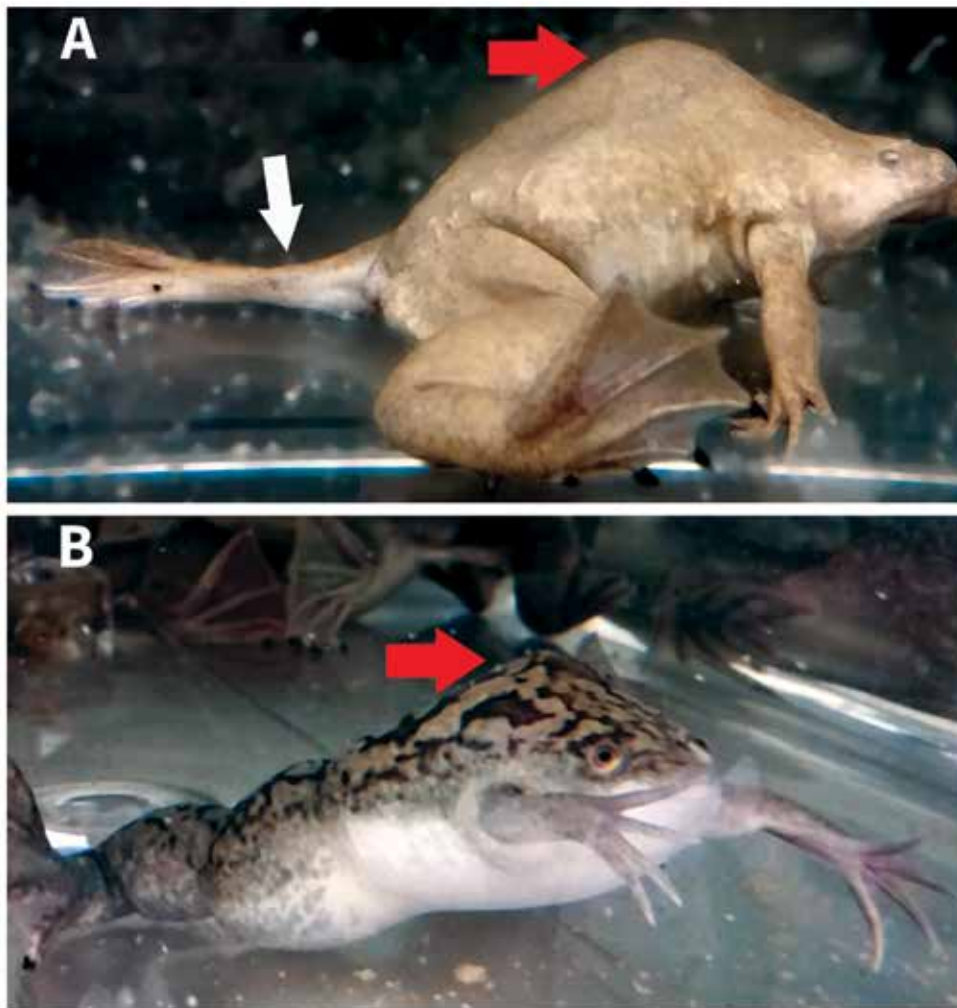
Figure 2. Two frogs displaying dorsal humps (red arrows) indicative of vertebral malformation, which represent this cohort's affected condition. Lateral view (enlarged 2×) of affected *X. tropicalis* (A) shows kyphosis and the abnormal positioning of the left rear leg due to coxofemoral subluxation (white arrow). Lateral view of an affected *X. laevis* (B). No other skeletal abnormalities grossly visible.

procedures; however, these conditions have periodically appeared in individuals in this colony over the last several years.

Animal Husbandry. Housing systems, husbandry and tadpole rearing protocols were adapted from those described by others.[34,54] Tadpoles were staged as described previously.[13,35] Hatched tadpoles were fed finely ground frog brittle (Nasco, Ft Atkinson, WI) twice daily and reared at approximately 21 °C for *X. laevis* and approximately 26 °C for *X. tropicalis* with a 10% daily water change. Animals were housed in a X-Hab 3-tier XR4 (40 L tanks) or 2-tier XR5 (75 L tanks) recirculating system (Pentair Aquatic Eco Systems, Cary, NC), using RO treated water reconstituted with Sea Marine Mix (Marine Enterprises International, LCC, Baltimore, MD). Water in the housing system was filtered using 120 µm filter pads and combined moving and submerged bed biologic filtration, followed by 50 µm pleated filter cartridges and filtration over activated carbon to adsorb volatile organics and other contaminants. UV light was used for disinfection, at a dose of 110 mJ/cm² at the end of the lamp life (approximately 12 mo).

The housing system water was supplemented weekly with Na bicarbonate and Ca carbonate powder, replaced as needed to maintain an osmolality of 400 to 800 µS at 21 to 27 °C, with a pH 7.0 to 7.5 (monitored weekly). Water quality parameters were tested monthly (more often if needed) using spectrophotometric

and colorimetric tests and maintained within the following ranges: ammonia (0 to 1.00 mg/L), nitrite (0 to 0.5 mg/L), nitrate (0 to 50 mg/L), chlorine (0 ppm). Total gas pressure (95% to 100%) was measured continuously using an in-line meter (Aquatic Habitats Sentinel, Pentair Aquatic Ecosystems, Apopka, FL).

All frogs of both species were housed in clear plastic tanks. Sexually mature, adult *X. laevis* were also housed in static, non-recirculating 20L tanks. The water in the adult *X. laevis* static tanks was conditioned RO treated water as described above and was maintained at 20 to 22 °C with a pH of 7.0 to 7.5. All water quality parameters were monitored as described above, and the water completely changed 3 times each week. The room that housed both species had a light cycle of 12 h on/12 h off. The tank stocking density was as follows: 50 tadpoles/L at NF stages[35] 42 to 52, 5 tadpoles/L at NF stages 52 to 66, 3 juvenile froglets/L (snout-to-vent length (SVL), 25 to 50 mm), one adult, sexually mature *X. laevis* (SVL 80 to 110 mm)/2.5 L and one adult *X. tropicalis* (SVL 40 to 50 mm)/0.75 L. Male and female frogs were housed in the same tank. All frogs were fed Nasco frog brittle (Nasco, Ft Atkinson, WI) of the nutritional formula and size appropriate for each developmental stage daily (or twice daily for a week for newly hatched tadpoles). Adult frogs (at approximately 3 to 6 mo of age for *X. tropicalis* and 2 to 3 y of age for *X. laevis*), were fed once a day on Mondays, Wednesdays
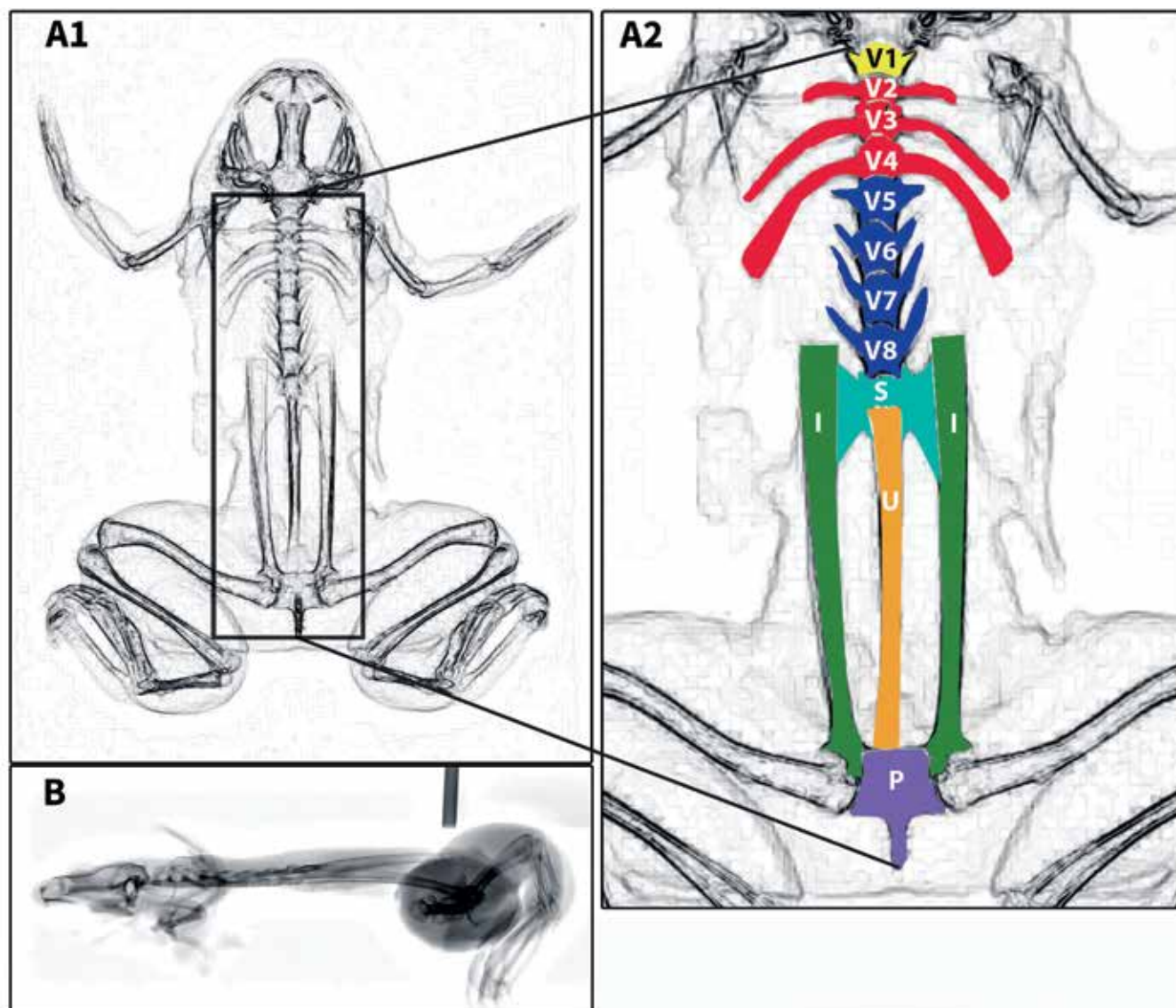
Figure 3. Ventrodorsal (A1–A2) and right lateral (B) inverted-grayscale radiographs of a control *X. laevis*. Important axial skeletal features shown with color-coded labeling (A2). Amphibian vertebrae numbers and structure differ significantly from the typical mammalian vertebral column. The normal *Xenopus* spp. vertebral column is characterized (from cranial to caudal) by: the atlas (a single cervical vertebra, V1, shown in yellow), 3 vertebrae with elongated transverse processes (V2–V4) shown in red, 4 vertebrae with transverse processes (V5–V8) shown in blue, a sacrum (S) shown in teal with bilateral sacral transverse processes that attach to the elongated ilial shafts (I). The ilial shafts and the ilial portion of the coxofemoral joint are shown in green. The urostyle (U) composed of fused coccygeal vertebrae is shown in orange. Ilial shafts connect to the rest of the pelvis (P) shown in purple consisting of fused pubis, ischium, and the remainder of the ilium. Note the normal, flattened skull and straight plane of the axial skeleton in B.

and Fridays. The frogs were monitored daily by the laboratory and veterinary staff for signs of injury or disease.

Xenopus spp. Colony History. The affected *Xenopus* spp. featured in this report include 6 sexually mature *X. laevis* approximately 2 to 3 y old (3 males, 3 females), and 4 sexually mature female *X. tropicalis* approximately 6 mo to 1 y-old. All affected frogs were observed in their housing tanks to have a range of axial skeleton malformations with varying degrees of kyphosis and scoliosis (Figure 2). The 10 affected frogs examined in this report came from a colony of approximately 200 genetically modified frogs, produced over a 3-y period by this laboratory. Genetic monitoring was limited to checking for transgenic fluorescent protein expression under a fluorescence dissecting microscope. The adult *X. laevis* founders came from Nasco (Nasco, Ft Atkinson, WI). *X. tropicalis* founders were transferred from another laboratory that has not reported skeletal malformations in their colonies. Health checks were performed daily. Because the animals were observed to be healthy, we did not evaluate for pathogens. Gross deformities were observed in these frogs at the juvenile froglet stage or older. Upon physical examination, all frogs were healthy and able to swim, although some frogs swam spastically, or seemed to have difficulty swimming to the water's surface. The affected frogs were otherwise in good body condition, able to eat, and had a history of good egg and oocyte production, as did the unaffected frogs in their tanks.

Imaging Procedures. All affected frogs described in this report were removed from the colony and humanely euthanized by immersion in buffered 0.5% tricaine methanosulfate (MS222, Thermo-Fisher, Waltham, MA) to effect (30 min or more immersion; death confirmed by lack of response to toe pinch). The formalin-fixed carcasses were submitted to Stanford University for further evaluation: radiographs, computed tomography,
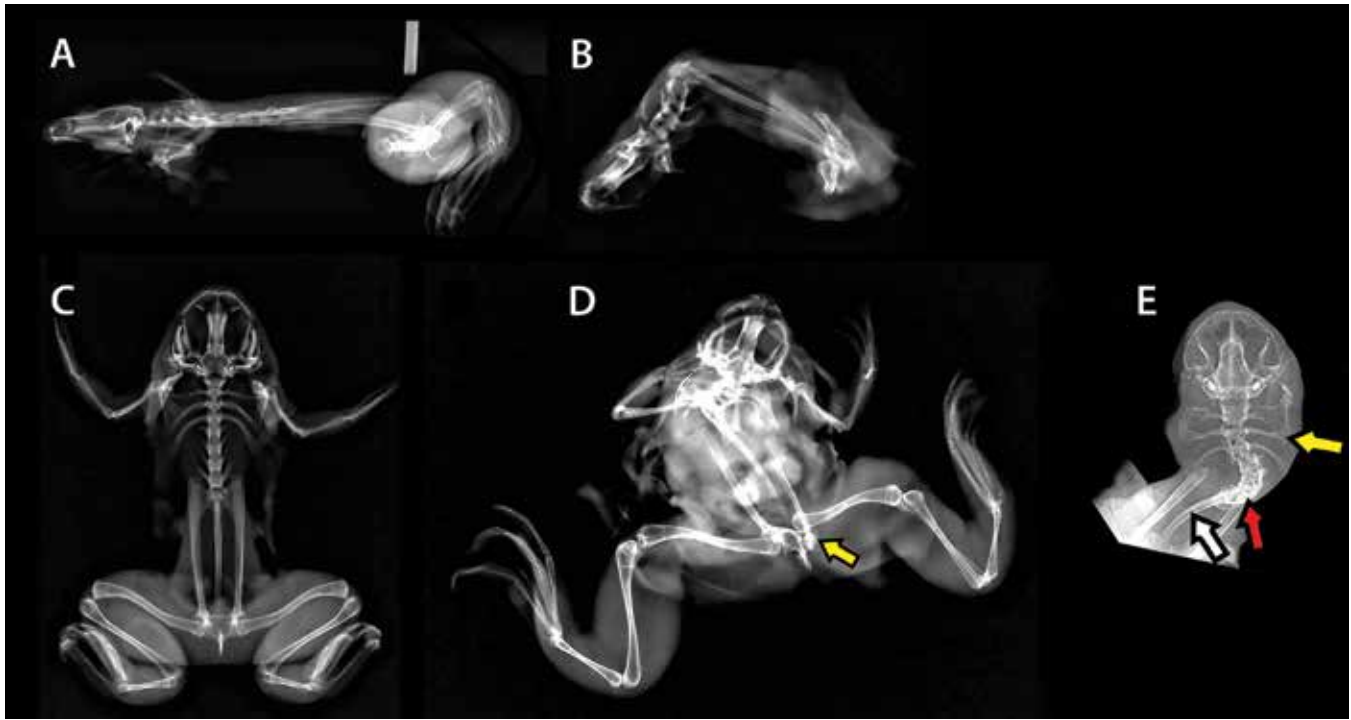
Figure 4. Right lateral radiographs of a control *X. laevis* (SVL approximately 110 mm) (A) and an affected *X. laevis* (SVL approximately 50 mm) (B) with severe kyphosis. Ventrodorsal view of a control *X. laevis* (C). Ventrodorsal views of an affected *X. laevis* showing scoliosis and coxofemoral luxation (yellow arrow) (D), and another affected *X. laevis* showing scoliosis focused in the presacral vertebrae (red arrow), with misshapen transverse processes (yellow arrow) and a curved urostyle (white arrow). The normal appendages are not shown on the *X. laevis* in E to enhance radiographic details that were otherwise difficult to discern.

gross necropsy, and histopathology. Right lateral and multiple ventrodorsal and/or dorsoventral radiographs as necessary due to the distorted anatomy of 6 affected frogs (4 *X. laevis* and 2 *X. tropicalis*) and a control *X. laevis* were obtained at 80 kVp and 3.5 mAs using a Sedecal APR-VET generator (Sedecal Vet Ray Technology, Arlington Heights, IL) and a digital radiograph plate (Smart DR 1717G, Sound Technologies, Carlsbad, CA). Computed tomography (CT) scans were obtained from 4 affected frogs (2 *X. laevis* and 2 *X. tropicalis*) and 4 unaffected frogs as controls (3 wildtype adult female *X. laevis* and 1 wildtype *X. tropicalis* from the colony). All *Xenopus* spp. scans were performed on a preclinical PET/CT scanner at 80 kV and 500 uA with slice thickness 103 µm, 1024 by 1024 matrix, and 103 µm in plane pixel dimensions (Siemens Inveon PET/CT, Siemens Medical Solutions, Malvern, PA). Projection images acquired by the Inveon MicroCT scanner were then reconstructed to a 3D dataset using the Inveon Acquistion Workplace platform (Siemens Medical Solutions, Malvern, PA). CT images were evaluated using multiplanar reconstructions in Horos (Horosproject. org, Nimble LLC d/b/a Purview, Annapolis, MD) and 3D renderings generated from the CT data with Amira 6.0 software (Thermo-Fisher, Waltham, MA). Snout-to-vent length (SVL) measurements were performed using Horos (Horosproject.org, Nimble LLC d/b/a Purview, Annapolis, MD), from a sagittal plane reformat along the longest line from the tip of the snout to the termination of the soft tissues on midline caudal to the pelvis.

Necropsy and Histology. Complete necropsies were performed on all affected frogs and one normal control frog. Vertebral columns were dissected free from skeletal muscles and the appendicular skeleton. The vertebral columns were postfixed and decalcified in CA-Ex II (Fischer Scientific, Upland, CA), then sectioned along the sagittal plane and routinely processed

for paraffin embedding and staining of slides with Hematoxylin and Eosin (H and E). Slides were examined by a Board Certified Veterinary Pathologist (DMB).

Results
Radiographic Findings. Right lateral radiographs and multiple ventrodorsal and/or dorsoventral radiographs of the whole body were obtained for 6 affected frogs (3 *X. laevis,* 3 *X. tropicalis*) and a control frog (*X. laevis*). To assist with anatomic interpretation of the radiographs, skeletal features of a control frog are shown in an inverted-grayscale radiograph (Figure 3). The *Xenopus* spp. axial skeleton is composed of a skull, 8 presacral vertebrae, which in the mature frog have elongated transverse processes on vertebrae 2 through 4 (sometimes referred to as "ribs"), a sacrum that attaches to ilial wings, and a urostyle.

Kyphoscoliosis was present in all frogs, with the misalignment originating from malformed vertebrae (Figure 4). In addition, segmentation defects and transverse process malformations were seen in the presacral vertebrae. Although difficult to discern, the sacral transverse processes did not appear to articulate with the ilial wings in multiple *X. laevis* and *X. tropicalis*, and a normal sacroiliac joint was not radiographically identifiable. Radiographs also revealed coxofemoral luxation in one frog. Due to severe kyphosis and scoliosis, even with multiple orthogonal projections, the full extent of the skeletal abnormalities could not be discerned on radiographs.

Computed Tomography and 3D Reconstruction of the Skeleton. Computed tomography and 3D reconstructions of the CT data were used to more clearly visualize defects in the axial skeletons of 4 affected frogs (2 *X. laevis,* 2 *X. tropicalis*) and a control frog (*X. laevis*). These 3D reconstructions can be viewed in Figures S1 through S5. Selected 3D reconstruction images of

Figure 5. Images of 3D reconstructions of the osseous structures derived from the CT scans of the axial skeleton at 90-degree rotations; control *X. laevis* in top row (A), affected *X. laevis* (Frog 5) below (B). Scoliosis, kyphosis, transverse process malformation including of the sacral vertebrae, and torsional/rotational deformities centered most often on the V5–V8 presacral vertebrae with variable segmentation defects (for example, commonly V1-V2 fusion). Full 3D rotation shown in Figure S2.

an affected *X. laevis* (Figure 5) show lesions typical of frogs in this report: kyphosis, scoliosis, incomplete vertebral segmentation, malformation of the transverse processes and curving or shortening of the urostyle. In the 2 severely affected *X. laevis*, a normal sacroiliac articulation was not identified, and the sacral transverse processes were malformed. One of these *X. laevis* also had unilateral coxofemoral subluxation. Detailed descriptions of the skeletal abnormalities in these 4 scanned frogs are provided in the skeletal abnormality summary table (Figure 6). Skeletal abnormalities determined by imaging were confirmed at necropsy.

The SVL is typically used to estimate the age and sex of *Xenopus* spp., but was notably shorter in these frogs, as measured on the CT scans. The SVL of one of the most severely affected female *X. laevis* was measured at 47 mm, in contrast to a control female *X. laevis*, which had a SVL measurement of 95 mm (the normal range for laboratory *X. laevis* is 80 to 110 mm).[18] The SVL of 2 female *X. tropicalis* with mild kyphosis was 49 mm, which falls within the normal range of SVL measurements for a control female *X. tropicalis* (40 to 50 mm).[18]

Gross Necropsy and Histopathology. Aside from lesions involving the vertebral column and/or other parts of the axial skeleton, gross lesions were not apparent in any of these frogs. Viscera and skin appeared grossly normal and showed no evidence of histopathologic lesions. There was no evidence of parasitic infestation or infectious disease. The malformations and anomalies observed at necropsy in the axial skeletons of all 10 frogs are summarized in Figure 6. Due to the tortuous

nature of the vertebral columns, orientation for histologic evaluation was less than ideal. However, sections of bone, joints, and soft tissues clearly demonstrate that histologic lesions in these frogs were prominent in the intervertebral joints. Figure 7 shows representative photomicrographs of normal and affected frogs. Figure 7 A is representative of a normal vertebral column and spinal cord with normal histoarchitecture of the intervertebral joints (that is, smooth articular cartilage, evenly spaced and appropriately conforming (concave/convex) joint halves). Figures 7 B through D depict histology of an affected frog with a range of lesions, including: misshapen intervertebral joints with nonconforming articular surfaces, narrowed joint cavities, flattened or irregularly formed articular cartilage, chondrocytes that lacked polarity, excess fibrocartilage, and evidence of irregular bone resorption and remodeling. No lesions were noted in any aspect of any of the frogs' spinal cords, including gray matter, white matter, central canal, or dorsal root ganglia.

Discussion

This is the first report, to our knowledge, of axial skeletal malformations in adult genetically modified laboratory *Xenopus* spp., and the first report using 3D reconstruction of CT scans as a diagnostic tool. Together, the gross examination, imaging studies, and histologic examination of these frogs revealed common abnormal skeletal features: kyphosis, kyphoscoliosis, vertebral segmentation defects, sacral/sacroiliac joint malformation,

Frog ID number	Species and Sex (M/F)	V1	Vertebrae with elongated transverse processes (V2 – V4)	Vertebrae with transverse processes (V5 – V8)	Sacrum and Urostyle	Pelvis	General Curvature
1	*X. laevis* M	Fused to V2	Incomplete segmentation with malformed elongated transverse processes	Scoliosis and kyphosis; incomplete segmentation	Normal	Normal	Severe scoliosis and kyphosis centered on V5-V8; segmentation defect and malformed transverse processes; block vertebrae
2	*X. laevis* M	Normal	Mild scoliosis	Severe kyphosis and scoliosis	Sacrum not connected to ilium; urostyle short and/or incompletely ossified	Pelvis incompletely ossified	Severe scoliosis and kyphosis centered at V5-V8; mild scoliosis in opposite direction at V2-V4; incomplete ossification of ilium and sacrum not connected
3	*X. laevis* M	Normal	Malformed elongated transverse processes	Severe scoliosis and kyphosis	Sacrum not connected to ilium	Unilateral coxofemoral luxation	Severe kyphosis and scoliosis; sacrum not connected to ilium
4	*X. laevis* F	V1-V2 fused	Malformed elongated transverse processes	Severe scoliosis and kyphosis centered at V5-V8	Unilateral attachment of sacrum to ilium; urostyle curved	Normal	Severe kyphosis and scoliosis centered on V5-V8; unilateral sacral attachment to ilium; segmentation defects; block vertebrae
5*	*X. laevis* F	V1-V2 fused	Malformed elongated transverse processes	Severe scoliosis, kyphosis, and torsional deformity	Sacrum not connected to ilium; urostyle short	Unilateral coxofemoral subluxation	Severe kyphosis, scoliosis and torsional deformity centered on V5-V8; segmentation defects; block vertebrae
6*	*X. laevis* F	V1-V2 fused	Malformed elongated transverse processes	Scoliosis, kyphosis, and torsional deformity	Sacrum not connected to ilium; urostyle short and curved	Normal	Severe kyphosis, scoliosis, and torsional deformity centered on V5-V8; segmentation defects; block vertebrae
7	*X. tropicalis* F	V1-V3 fused	Incomplete segmentation	Scoliosis and kyphosis centered on V8 and the sacrum	Normal	Normal	Severe scoliosis and kyphosis centered on V8 and sacrum; segmentation defects; block vertebrae
8	*X. tropicalis* F	V1 fused to skull/occiput and V2	Incomplete segmentation	Severe scoliosis and kyphosis centered here with questionable segmentation	Sacrum not connected to ilium; urostyle curved	Normal	Severe kyphosis and scoliosis centered on V5-V8; sacrum not connected to ilium; urostyle curved; segmentation defects; block vertebrae
9*	*X. tropicalis* F	Normal	Normal	Focal kyphosis	Normal	Normal	Mild kyphosis centered on V5-V8
10*	*X. tropicalis* F	Normal	Normal	Focal kyphosis	Normal	Normal	Mild kyphosis centered on V5-V8

Figure 6. Summary of radiographic, CT scan, and necropsy findings. Asterisk (*) indicates individual was CT scanned (see Figures S2 through S5 for corresponding 3D rotation videos).

sacral and thoracic transverse process malformations, urostyle malformations, and coxofemoral subluxation. Despite the severely malformed vertebrae, the spinal cord of affected animals was not adversely affected. All frogs described in this report had reached sexual maturity, were able to eat and swim, and were otherwise in robust health.

This laboratory maintained this frog colony for investigation into thyroid hormone receptor function and gene expression and regulation. However, whether the induction and expression of mutant *THRA*, a gene that encodes the thyroid hormone receptor THRA1, in these frogs contributed to the axial skeletal malformations is uncertain. Mutation of *THRA*, the gene that encodes the thyroid hormone receptor THRA1, has been previously shown to result in scoliosis, misshapen vertebrae, and congenital hip dislocation in both human patients and mice.[5,17] Similarly, insertion of transgenes into *Xenopus* spp. embryos, specifically those that involve disruption of the thyroid hormone pathways, have been shown to cause developmental abnormalities[8] although not kyphosis, scoliosis, or any of the other skeletal malformations described in this report. Nevertheless, the induction and expression of transgenes, inactivation (knockout) of existing genes by insertional mutagenesis, or spontaneously occurring or experimentally induced variants of *THRA* and their expression cannot be excluded as a possible cause of the phenotype reported here.

The laboratory maintaining these frogs used well-established, standard protocols to inject frog eggs and embryos with nucleic acids and other organic substances.[13,43] TALEN injections, REMI and meganuclease induced transgenesis methods have been used in frogs for the past decade or so, but no past publication has associated these methodologies with unanticipated skeletal malformations. Nevertheless, physical manipulation or other experimental conditions could contribute to the development of the skeletal abnormalities. Embryo dejellying, the stage at which microinjections were performed, microinjection volume or concentration, possible transgene contamination, or unidentified variables in the macro- or microenvironmental conditions during manipulation may have contributed to the etiopathogenesis.[36,39]

This colony had no history of infectious or parasitic disease, and none were detected in any of the affected frogs at necropsy. The frogs in this report were reared and maintained using standard housing and husbandry practices typical for laboratory *Xenopus* spp.[34,54] Exposure of these frogs to pesticides or toxins, or to substances that have been associated with skeletal deformities, is unlikely.[3,21,24,41,53] However, the RO treated water source supplying the *Xenopus* spp. housing systems in this laboratory was not screened for water toxicants, such as perfumes, lotions, cleaning substances, herbicides, pesticides or heavy metals. Thus, water pollution with these agents (or others) cannot be ruled out as the cause of the skeletal abnormalities. However, given the low incidence of this condition within the colony, and the long history of the colony's overall good health, exposure to water toxicants seems unlikely.

The skeletal malformations observed in the frogs reported here are probably due to complex interactions between many variables, including the genetic background of the frogs. This condition may also occur naturally but rarely in wild populations of *Xenopus* spp.. We speculate that the severity of kyphoscoliosis would impede wild *Xenopus* spp. in taking cover in the
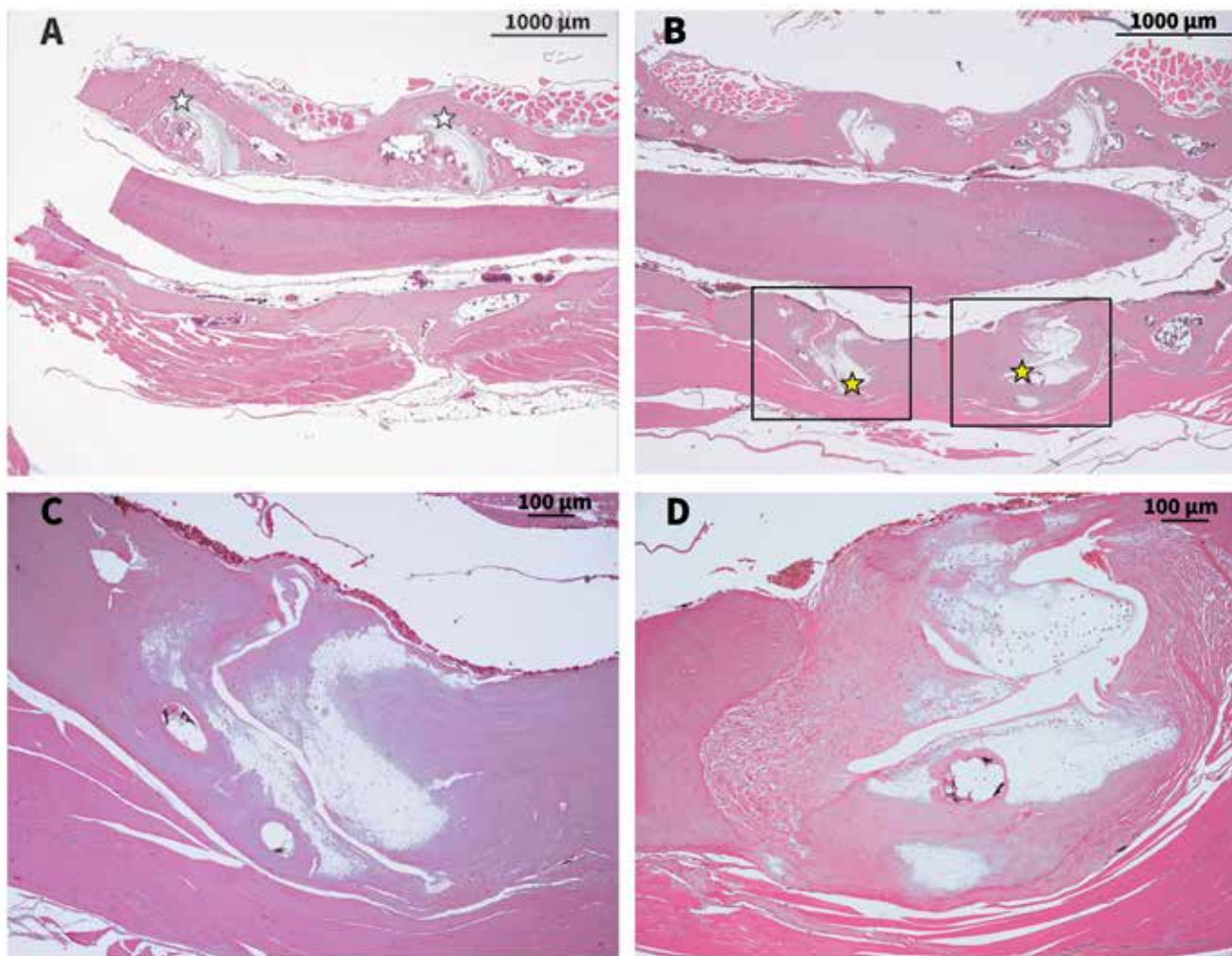
Figure 7. Representative photomicrographs of intervertebral joints: White star indicates normal joint; scale bar 1000 μm (A). Yellow star indicates abnormal joint, scale bar 1000 μm (B). Higher magnification of abnormal joints in Figure 7 B (C and D). Scale bar 100 μm. All slides stained with H and E.

narrow crevices between rocks and similar shelters, which is their primary means of defense against predation.

Supplementary Materials

Figure S1. Wildtype *X. laevis*: 3D rendering of osseous structures from CT scans. The skeleton is bilaterally symmetrical, and vertebrae are aligned in both the dorsal and sagittal planes. This normal adult *X. laevis* skeleton is representative of the normal *X. tropicalis* skeleton too, though *X. tropicalis* is generally smaller.

Figure S2. *X. laevis* (Frog 5): 3D rendering of osseous structures from CT scans. Axial skeletal abnormalities in this adult individual are described by Figure 5 B and include V1–V2 fusion, malformed transverse processes, scoliosis, kyphosis, and a torsional deformity of the vertebral column. The sacrum does not have an osseous connection to the ilium due to sacral transverse process malformation including a torsional component.

Figure S3. *X. laevis* (Frog 6): 3D rendering of osseous structures from CT scans. Axial skeletal abnormalities in this adult include severe kyphoscoliosis, malformed elongated transverse processes, and a shortened and curved urostyle. The sacrum does not have an osseous connection to the ilium due to sacral transverse process malformation including a torsional component.

Figure S4. *X. tropicalis* (Frog 9): 3D rendering of osseous structures from CT scans. Hunchback in this adult individual is due to mild kyphosis centered on V5–V8.

Figure S5. *X. tropicalis* (Frog 10): 3D rendering of osseous structures from CT scans. Hunchback in this adult individual shows is due to mild kyphosis centered on V5–V8.

Acknowledgments

References

1. **Arbuatti A, Della Salda L, Romanucci M.** 2013. Spinal deformities in a wild line of *Poecilia wingei* bred in captivity: Report of cases and review of the literature. Asian Pac J Trop Biomed **3:**186–190. https://doi.org/10.1016/S2221-1691(13)60047-7.

2. **Aztekin C, Hiscock TW, Marioni JC, Gurdon JB, Simons BD, Jullien J.** 2019. Identification of a regeneration-organizing cell in the *Xenopus* tail. Science **364:**653–658. https://doi.org/10.1126/science.aav9996.

3. **Bacchetta R, Mantecca P, Andrioletti M, Vismara C, Vailati G.** 2008. Axial-skeletal defects caused by carbaryl in *Xenopus laevis* embryos. Sci Total Environ **392:**110–118. https://doi.org/10.1016/j.scitotenv.2007.11.031.

4. **Baker TR, Peterson RE, Heideman W.** 2014. Using zebrafish as a model system for studying the transgenerational effects of dioxin. Toxicol Sci **138:**403–411. https://doi.org/10.1093/toxsci/kfu006.

5. **Bassett JHD, Williams GR.** 2016. Role of thyroid hormones in skeletal development and bone maintenance. Endocr Rev **37:**135–187. https://doi.org/10.1210/er.2015-1106.

6. **Bisland SK, Johnson C, Wilson BC, Burch S.** [Internet]. 2009. Effect of VEGF expression on vertebral growth plates following hypoxic stress. Orthop Proc **91-B.** [Cited 21 February 2018]. Available at: https://online.boneandjoint.org.uk/doi/abs/10.1302/0301-620X.91BSUPP_II.0910225c.

7. **Buchholz DR, Paul BD, Fu L, Shi YB.** 2006. Molecular and developmental analyses of thyroid hormone receptor function in *Xenopus laevis*, the African clawed frog. Gen Comp Endocrinol **145:**1–19. https://doi.org/10.1016/j.ygcen.2005.07.009.

8. **Buchholz DR, Shi Y-B.** 2018. Dual function model revised by thyroid hormone receptor alpha knockout frogs. Gen Comp Endocrinol **265:**214–218. https://doi.org/10.1016/j.ygcen.2018.04.020.

9. **Buchholz DR, Tomita A, Fu L, Paul BD, Shi Y-B.** 2004. Transgenic analysis reveals that thyroid hormone receptor is sufficient to mediate the thyroid hormone signal in frog metamorphosis. Mol Cell Biol **24:**9026–9037. https://doi.org/10.1128/MCB.24.20.9026-9037.2004.

10. **Cai L, Das B, Brown DD.** 2007. Changing a limb muscle growth program into a resorption program. Dev Biol **304:**260–271. https://doi.org/10.1016/j.ydbio.2006.12.031.

11. **Castro Sánchez R, Bustos Obregón E, Rojas Rauco M.** 2012. Vertebral column deformity and hypoxia in *Salmo Salar*. Int J Morphol **29:**1291–1295. https://doi.org/10.4067/S0717-95022011000400036.

12. **Chesneau A, Sachs LM, Chai N, Chen Y, Du Pasquier L, Loeber J, Pollet N, Reilly M, Weeks DL, Bronchain OJ.** 2008. Transgenesis procedures in *Xenopus*. Biol Cell **100:**503–521. https://doi.org/10.1042/BC20070148.

13. **Choi J, Suzuki KT, Sakuma T, Shewade L, Yamamoto T, Buchholz DR.** 2015. Unliganded thyroid hormone receptor α regulates developmental timing via gene repression in *Xenopus tropicalis*. Endocrinology **156:**735–744. https://doi.org/10.1210/en.2014-1554.

14. **Das B, Brown DD.** 2004. Controlling transgene expression to study *Xenopus laevis* metamorphosis. Proc Natl Acad Sci U S A **101:**4839–4842. https://doi.org/10.1073/pnas.0401011101.

15. **Dayer R, Haumont T, Belaieff W, Lascombes P.** 2013. Idiopathic scoliosis: etiological concepts and hypotheses. J Child Orthop **7:**11–16. https://doi.org/10.1007/s11832-012-0458-3.

16. **Eissa AE, Moustafa M, El-Husseiny IN, Saeid S, Saleh O, Borhan T.** 2009. Identification of some skeletal deformities in freshwater teleosts raised in Egyptian aquaculture. Chemosphere **77:**419–425. https://doi.org/10.1016/j.chemosphere.2009.06.050.

17. **Espiard S, Savagner F, Flamant F, Vlaeminck-Guillem V, Guyot R, Munier M, d'Herbomez M, Bourguet W, Pinto G, Rose C, Rodien P, Wemeau JL.** 2015. A novel mutation in THRA gene associated with an atypical phenotype of resistance to thyroid hormone. J Clin Endocrinol Metab **100:**2841–2848. https://doi.org/10.1210/jc.2015-1120.

18. **Green SL.** 2010. The laboratory *Xenopus* sp. Boca Raton (FL): CRC Press.

19. **Hardwick LJA, Philpott A.** 2015. An oncologist's friend: How *Xenopus* contributes to cancer research. Dev Biol **408:**180–187. https://doi.org/10.1016/j.ydbio.2015.02.003.

20. **Hayes M, Gao X, Yu L, Paria N, Henkelman M, Wise C, Ciruna B.** 2014. *Ptk7* mutant zebrafish models of congenital and idiopathic scoliosis implicate dysregulated Wnt signalling in disease. Nat Commun **5:**1–11. https://doi.org/10.1038/ncomms5777.

21. **Heimeier RA, Shi Y-B.** 2010. Amphibian metamorphosis as a model for studying endocrine disruption on vertebrate development: Effect of bisphenol A on thyroid hormone action. Gen Comp Endocrinol **168:**181–189. https://doi.org/10.1016/j.ygcen.2010.02.016.

22. **Hellsten U, Harland RM, Gilchrist MJ, Hendrix D, Jurka J, Kapitonov V, Ovcharenko I, Putnam NH, Shu S, Taher L, Blitz IL, Blumberg B, Dichmann DS, Dubchak I, Amaya E, Detter JC, Fletcher R, Gerhard DS, Goodstein D, Graves T, Grigoriev IV, Grimwood J, Kawashima T, Lindquist E, Lucas SM, Mead PE, Mitros T, Ogino H, Ohta Y, Poliakov AV, Pollet N, Robert J, Salamov A, Sater AK, Schmutz J, Terry A, Vize PD, Warren WC, Wells D, Wills A, Wilson RK, Zimmerman LB, Zorn AM, Grainger R, Grammer T, Khokha MK, Richardson PM, Rokhsar DS.** 2010. The genome of the Western clawed frog *Xenopus tropicalis*. Science **328:**633–636. https://doi.org/10.1126/science.1183670.

23. **Horb M, Wlizla M, Abu-Daya A, McNamara S, Gajdasik D, Igawa T, Suzuki A, Ogino H, Noble A, Centre de Resource Biologique Xenope team in France, Robert J, James-Zorn C, Guille M.** 2019. *Xenopus* resources: Transgenic, inbred and mutant animals, training opportunities, and web-based support. Front Physiol **10:**387–387. https://doi.org/10.3389/fphys.2019.00387.

24. **Iwamuro S, Sakakibara M, Terao M, Ozawa A, Kurobe C, Shigeura T, Kato M, Kikuyama S.** 2003. Teratogenic and antimetamorphic effects of bisphenol A on embryonic and larval *Xenopus laevis*. Gen Comp Endocrinol **133:**189–198. https://doi.org/10.1016/S0016-6480(03)00188-6.

25. **Jayawardena UA, Rohr JR, Navaratne AN, Amerasinghe PH, Rajakaruna RS.** 2016. Combined effects of pesticides and trematode infections on hourglass tree frog *Polypedates cruciger*. EcoHealth **13:**111–122. https://doi.org/10.1007/s10393-016-1103-2.

26. **Jayawardena UA, Tkach VV, Navaratne AN, Amerasinghe PH, Rajakaruna RS.** 2013. Malformations and mortality in the Asian common toad induced by exposure to *Pleurolophocercous cercariae* (*Trematoda: Cryptogonimidae*). Parasitol Int **62:**246–252. https://doi.org/10.1016/j.parint.2013.01.003.

27. **Kobayashi H, Watanabe T, Terashita N, Handa S, Furuno N.** 1989. Vertebral abnormalities following heat shock in *Xenopus* embryos. Dev Growth Differ **31:**65–70. https://doi.org/10.1111/j.1440-169X.1989.00065.x.

28. **Kroll KL, Amaya E.** 1996. Transgenic *Xenopus* embryos from sperm nuclear transplantations reveal FGF signaling requirements during gastrulation. Development **122:**3173–3183.

29. **Lasser M, Pratt B, Monahan C, Kim SW, Lowery LA.** 2019. The many faces of *Xenopus*: *Xenopus laevis* as a model system to study Wolf–Hirschhorn syndrome. Front Physiol **10:**1–12. https://doi.org/10.3389/fphys.2019.00817.

30. **Liu N, Niu J, Wang D, Chen J, Li X.** 2016. Spinal pathomorphological changes in the breeding giant salamander juveniles. Zoomorphology **135:**115–120. https://doi.org/10.1007/s00435-015-0292-5.

31. **Love NR, Chen Y, Bonev B, Gilchrist MJ, Fairclough L, Lea R, Mohun TJ, Paredes R, Zeef LAH, Amaya E.** 2011. Genome-wide analysis of gene expression during *Xenopus tropicalis* tadpole tail regeneration. BMC Dev Biol **11:**1–15. https://doi.org/10.1186/1471-213X-11-70.

32. **Martin BL, Kimelman D.** 2012. Canonical Wnt signaling dynamically controls multiple stem cell fate decisions during vertebrate body formation. Dev Cell **22:**223–232. https://doi.org/10.1016/j.devcel.2011.11.001.

33. **Martini A, Huysseune A, Witten PE, Boglione C.** 2020. Plasticity of the skeleton and skeletal deformities in zebrafish (*Danio rerio*) linked to rearing density. J Fish Biol Epub ahead of print:1–16. https://doi.org/10.1111/jfb.14272

34. **McNamara S, Wlizla M, Horb ME.** 2018. Husbandry, general care, and transportation of *Xenopus laevis* and *Xenopus tropicalis*. Methods Mol Biol **1865:**1–17. https://doi.org/10.1007/978-1-4939-8784-9_1.

35. **Nieuwkoop PD, Faber J.** 1967. Normal table of *Xenopus laevis* (Daudin). Amsterdam (Holland): North-Holland Publishing.

36. **Ogino H, McConnell WB, Grainger RM.** 2006. High-throughput transgenesis in *Xenopus* using *I-SceI* meganuclease. Nat Protoc **1:**1703–1710. https://doi.org/10.1038/nprot.2006.208.

37. **Ogino H, Ochi H.** 2009. Resources and transgenesis techniques for functional genomics in *Xenopus*. Dev Growth Differ **51:**387–401. https://doi.org/10.1111/j.1440-169X.2009.01098.x.

38. **Ouellet J, Odent T.** 2013. Animal models for scoliosis research: State of the art, current concepts and future perspective applications. Eur

Spine J **22 Suppl 2:**S81–S95. https://doi.org/10.1007/s00586-012-2396-7.

39. **Pan FC, Chen Y, Loeber J, Henningfeld K, Pieler T.** 2006. *I-SceI* meganuclease-mediated transgenesis in *Xenopus.* Dev Dyn **235:**247–252. https://doi.org/10.1002/dvdy.20608.

40. **Pathirana N, Meegaskumbura M, Rajakaruna R.** 2019. Host resistance and tolerance to parasitism: Development-dependent fitness consequences in common hourglass tree frog (*Polypedates cruciger*) tadpoles exposed to two larval trematodes. Can J Zool **97:**1021–1029. https://doi.org/10.1139/cjz-2018-0126.

41. **Plowman MC, Grbac-lvankovic S, Martin J, Hopfer SM, Sunderman FW Jr.** 1994. Malformations persist after metamorphosis of *Xenopus laevis* tadpoles exposed to Ni2+, Co2+, or Cd2+ in FE-TAX assays. Teratog Carcinog Mutagen **14:**135–144. https://doi.org/10.1002/tcm.1770140305.

42. **Pourquié O.** 2011. Vertebrate segmentation: From cyclic gene networks to scoliosis. Cell **145:**650–663. https://doi.org/10.1016/j.cell.2011.05.011.

43. **Rankin SA, Zorn AM, Buchholz DR.** 2011. New doxycycline-inducible transgenic lines in *Xenopus.* Dev Dyn **240:**1467–1474. https://doi.org/10.1002/dvdy.22642.

44. **Ruiz AM, Maerz JC, Davis AK, Keel MK, Ferreira AR, Conroy MJ, Morris LA, Fisk AT.** 2010. Patterns of development and abnormalities among tadpoles in a constructed wetland receiving treated wastewater. Environ Sci Technol **44:**4862–4868. https://doi.org/10.1021/es903785x.

45. **Sachs LM.** 2015. Unliganded thyroid hormone receptor function: Amphibian metamorphosis got TALENs. Endocrinology **156:**409–410. https://doi.org/10.1210/en.2014-2016.

46. **Sakuma T, Ochiai H, Kaneko T, Mashimo T, Tokumasu D, Sakane Y, Suzuki K-i, Miyamoto T, Sakamoto N, Matsuura S, Yamamoto T.** 2013. Repeating pattern of non-RVD variations in DNA-binding modules enhances TALEN activity. Sci Rep **3:**1–8. https://doi.org/10.1038/srep03379.

47. **Session AM, Uno Y, Kwon T, Chapman JA, Toyoda A, Takahashi S, Fukui A, Hikosaka A, Suzuki A, Kondo M, van Heeringen SJ, Quigley I, Heinz S, Ogino H, Ochi H, Hellsten U, Lyons JB, Simakov O, Putnam N, Stites J, Kuroki Y, Tanaka T, Michiue T, Watanabe M, Bogdanovic O, Lister R, Georgiou G, Paranjpe SS, van Kruijsbergen I, Shu S, Carlson J, Kinoshita T, Ohta Y, Mawaribuchi S, Jenkins J, Grimwood J, Schmutz J, Mitros T, Mozaffari SV, Suzuki Y, Haramoto Y, Yamamoto TS, Takagi C, Heald R, Miller K, Haudenschild C, Kitzman J, Nakayama T, Izutsu Y, Robert J, Fortriede J, Burns K, Lotay V, Karimi K, Yasuoka Y, Dichmann DS, Flajnik MF, Houston DW, Shendure J, DuPasquier L, Vize PD, Zorn AM, Ito M, Marcotte EM, Wallingford JB, Ito Y, Asashima M, Ueno N, Matsuda Y, Veenstra GJC, Fujiyama A, Harland RM, Taira M, Rokhsar DS.** 2016. Genome evolution in the allotetraploid frog *Xenopus laevis.* Nature **538:**336–343. https://doi.org/10.1038/nature19840.

48. **Slater PG, Hayrapetian L, Lowery LA.** 2017. *Xenopus laevis* as a model system to study cytoskeletal dynamics during axon pathfinding. Genesis **55:**1–11.

49. **Sparrow DB, Latinkic B, Mohun TJ.** 2000. A simplified method of generating transgenic *Xenopus.* Nucleic Acids Res **28:**1–4. https://doi.org/10.1093/nar/28.4.e12.

50. **Vize PD, Zorn AM.** 2017. *Xenopus* genomic data and browser resources. Dev Biol **426:**194–199. https://doi.org/10.1016/j.ydbio.2016.03.030.

51. **Warkman AS, Krieg PA.** 2007. *Xenopus* as a model system for vertebrate heart development. Semin Cell Dev Biol **18:**46–53. https://doi.org/10.1016/j.semcdb.2006.11.010.

52. **Wen L, Shi Y-B.** 2014. Unliganded thyroid hormone receptor α controls developmental timing in *Xenopus tropicalis.* Endocrinology **156:**721–734. https://doi.org/10.1210/en.2014-1439.

53. **Wheeler GN, Brändli AW.** 2009. Simple vertebrate models for chemical genetics and drug discovery screens: Lessons from zebrafish and *Xenopus.* Dev Dyn **238:**1287–1308. https://doi.org/10.1002/dvdy.21967.

54. **Wlizla M, McNamara S, Horb ME.** 2018. Generation and care of *Xenopus laevis* and *Xenopus tropicalis* embryos. Methods Mol Biol **1865:**19–32. https://doi.org/10.1007/978-1-4939-8784-9_2.